CHIN. PHYS. LETT. Vol. 37, No. 6 (2020) 068502

Effect of a Single Threading Dislocation on Electrical and Single Photon Detection Characteristics of 4H-SiC Ultraviolet Avalanche Photodiodes *

Lin-Lin Su(苏琳琳), Dong Zhou(周东)**, Qing Liu(刘清), Fang-Fang Ren(任芳芳), Dun-Jun Chen(陈敦军), Rong Zhang(张荣), You-Dou Zheng(郑有炓), Hai Lu(陆海)**

School of Electronic Science and Engineering, Nanjing University, Nanjing 210023, China

(Received 16 March 2020)

We fabricated 4H-SiC ultraviolet avalanche photodiode (APD) arrays and systematically investigated the effect of threading dislocations on electrical and single photon detection characteristics of 4H-SiC APDs. Based on a statistical correlation study of individual device performance and structural defect mapping revealed by molten KOH etching, it is determined with high confidence level that even a single threading dislocation within APD active region would lead to apparent device performance degradation, including increase of dark current near breakdown voltage, premature breakdown and reduction of single photon detection efficiency at fixed dark count rate.

PACS: 85.30.De, 85.60.Gz, 85.60.Dw, 85.60.Bt DOI: 10.1088/0256-307X/37/6/068502

Detection of weak ultraviolet (UV) light is imperative in many critical civilian and scientific research applications such as corona discharge detection, environmental monitoring, UV astronomy, biological and chemical agent detection.[1–5] As an attractive candidate for weak UV signal detection, avalanche photodiodes (APDs) operating in Geiger mode exhibit promising performance, including small size, low dark current and high multiplication gain.[6–8] Compared with other wide bandgap semiconductors, 4H-SiC represents an excellent candidate for UV detection due to its relatively mature material growth and processing technologies.[9,10] Although 6-inch conductive n-type 4H-SiC substrates have become the mainstream of power device fabrication, SiC wafers still contain a variety of defects such as basal plane dislocations (BPDs), threading dislocations (TDs) and point defects. Micro-pipes are usually taken as major killer defects for SiC devices, but their density has dropped to less than $0.01\,\mathrm{cm}^{-2}$ for 6-inch SiC substrates.[11] Nowadays, the density of TDs has been reduced to $10^3\,\mathrm{cm}^{-2}$ level for 4H-SiC epi-wafers, which is much lower than that of GaN, another wide bandgap semiconductor also being intensively investigated for UV detector applications. Currently, 4H-SiC is mainly studied and used for power device development. It is believed that compared with other structural defects, TDs in 4H-SiC have considerably less negative impact on the performance of power devices. Actually, during epitaxial growth, an important task is to convert very harmful BPDs to less harmful TDs.[12,13]

However, compared to conventional power devices, APDs work under much more demanding operation conditions. Specifically, they must continuously operate under critical electrical field (∼3.3 MV/cm), which may make the performance of SiC APDs more sensitive to structural defects within the device active region.[14] If this is the case, the risk of device degradation or even failure would increase fast at larger device size, resulting in poor device yield. Moreover, for future ultra-weak UV imaging applications, device yield and performance consistency are very important for realizing focal plane arrays based on SiC APDs. Until recently, there have been only several reports focusing on the impact of TDs on the performance of conventional SiC photodetectors which nevertheless work under low electrical field.[15,16] There are still few systematic studies on the correlation between TDs and single photon detection performance of SiC APDs. The purpose of this work is to investigate detailed impact of TDs on leakage current, breakdown voltage and single photon detection performance of 4H-SiC APDs.

In this work, multiple 1×128 SiC APD linear arrays have been fabricated to study the relationship between APD performance and TDs. As shown in Fig. 1(a), the SiC APD arrays are grown and fabricated on n-type 4H-SiC substrates. The epi-structure from bottom to top consists of a 5 μm n^+ layer ($N_D = 3 \times 10^{18}\,\mathrm{cm}^{-3}$), a 0.6 μm p^- multiplication layer ($N_A = 3 \times 10^{15}\,\mathrm{cm}^{-3}$), a 0.2 μm p contact layer ($N_A = 2 \times 10^{18}\,\mathrm{cm}^{-3}$) and a 0.2 μm p^+ cap layer ($N_A = 2 \times 10^{19}\,\mathrm{cm}^{-3}$). The fabrication process starts with mesa etching down to the multiplication layer by inductively coupled plasma etching with SF_6/O_2 as the etching gas. To suppress peak electrical field around device edge, beveled mesa with a slope angle of ∼6° is obtained based on a photoresist reflow technique.[17,18] The device surface is then passivated by thermal oxidation at 1050 ℃ in oxygen atmosphere followed by a 1 μm SiO_2 layer deposited by plasma-enhanced chemical vapor deposition at 350 ℃. After opening p contact holes by wet chemical etching, n-

*Supported by the National Key R&D Program of China under Grant No. 2016YFB0400902, the National Natural Science Foundation of China under Grant No. 61921005, and the Natural Science Foundation of Jiangsu Province under Grant No. BK20190302

**Corresponding authors. Email: hailu@nju.edu.cn; dongzhou@nju.edu.cn

© 2020 Chinese Physical Society and IOP Publishing Ltd

and p-type metal stacks both based on Ni/Ti/Al/Au (35 nm/50 nm/100 nm/100 nm) are deposited by e-beam evaporation. The devices are then annealed at 850 ℃ for 3 min in N_2 ambient by rapid thermal annealing. Finally, top p-contact pad based on Ti/Au bi-layer is deposited by e-beam evaporation. Figures 1(b) and 1(c) show the top-view images of an APD pixel and a whole 128-pixel APD linear array, respectively. Each APD pixel has a mesa diameter of 90 μm. The small size of the APDs resulted in the fact that most devices are dislocation-free or contain only one dislocation within the active region.

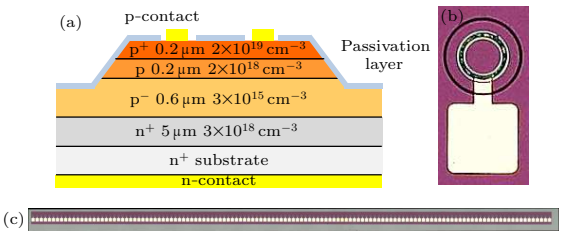

Fig. 1. Cross sectional schematic of the 4H-SiC APD device (a); top-view image of one APD pixel (b); top-view image of a complete 128-pixel SiC APD linear array (c).

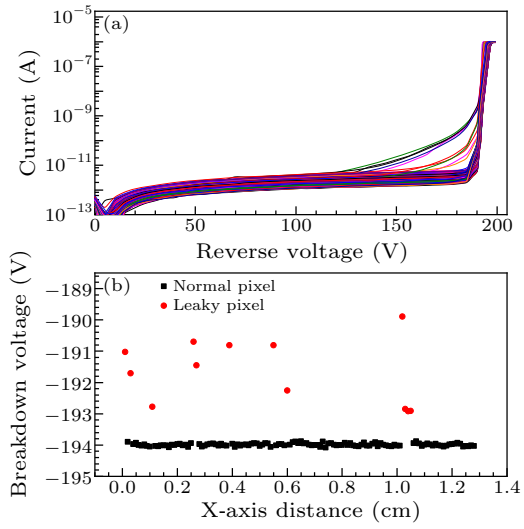

Fig. 2. (a) I–V curves of the complete 128 pixels within one linear array; (b) the distribution of breakdown voltage for one 128-pixel APD linear array.

The reverse current-voltage (I–V) curves of one complete 128-pixel SiC APD linear array are sequentially measured by using a semi-auto probe station. As shown in Fig. 2(a), the dark currents of these pixels remain at pA level when the reverse voltage is below 100 V. As bias further increases, the majority of pixels still exhibit steady low dark current before avalanche breakdown, while a few pixels indeed suffer from enhanced dark current of 1–2 orders of magnitude at high bias. Avalanche breakdown is signaled by a sharp increase of dark current and here breakdown voltage is defined at a dark current of 5×10^{-8} A. The breakdown voltage is found around 194 V for normal non-leaky pixels, while that of those leaky pixels is correspondingly lowered by 1–4 V. Figure 2(b) shows the distribution of breakdown voltages for the 128-pixel SiC APD linear array. Excluding leaky pixels, there is only about ±0.1 V breakdown voltage fluctuation across the whole linear array. The good consistency of breakdown voltage should be benefited from the uniform thickness and doping concentration of the multiplication layer across the epi-wafer.[19,20] It is found that there are totally 12 leaky pixels with reduced breakdown voltage within the 128-pixel APD linear array, corresponding to a device yield of 91%.

The single photon detection performances of the APD pixels are selectively measured by using a passive quenching circuit, in which a load resistor of 200 kΩ is used to quench the avalanche current. The voltage pulse signals are recorded by a high speed oscilloscope, which is in parallel connected to a 100 Ω sampling resistor. A 280 nm UV light emitting diode is used as light source and the calibrated incident UV photon flux is $\sim 1 \times 10^7$ photons/s. Figure 3 shows the dark count rate (DCR) of a representative normal pixel and several leaky pixels versus single photon detection efficiency (SPDE) at room temperature. It is found that the single photon detection performances of normal pixels are basically same, indicating good consistency. Specifically, when DCR is ∼3 Hz/μm^2, a room temperature SPDE of 3.2% can be obtained. However, at the same DCR, the leaky pixels exhibit lower SPDE as well as poor consistency. It is further observed that at the same SPDE, the higher the leakage current is, the higher the DCR is found among the leaky pixels. Thus, the poor single photon detection performance of leaky pixels further evidences that the enhanced dark current observed in those APD devices is not surface leakage but true leakage from p–n junctions.

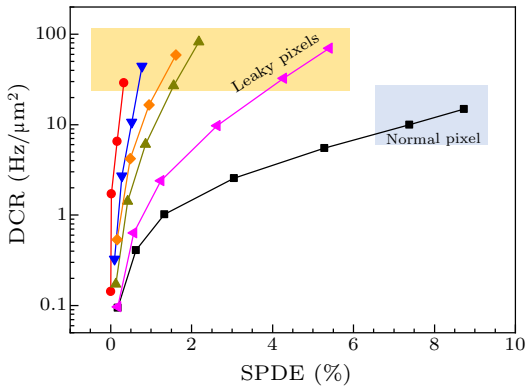

Fig. 3. The DCR of representative normal pixel and leaky pixels vs SPDE.

To identify the correlation between performance degradation and structural defects within the device active layer, up to 650 APD pixels of several linear arrays are sequentially characterized and labeled. These pixels are etched by aqua regia to remove metal contacts and then etched by molten KOH at 500 ℃ for 10 min to expose structural defects as etch pits. Inspection of wafer surface after etching is carried out

by an optical microscope and a scanning electron microscope (SEM). The type of structural defects can be identified based on the shape of etch pits. It is found that over 99% of the exposed defects are TDs corresponding to hexagonal etch pits while the rest are BPDs corresponding to oval-shaped etch pits. The density of TDs is $\sim 2 \times 10^3\,\mathrm{cm}^{-2}$ for the SiC epi-wafer and all etch pits found on APD surface are TDs. Although normally the etch pit size of threading screw dislocations (TSDs) is slightly larger than that of threading edge dislocations (TEDs) in 4H-SiC, in this work it is difficult to definitely distinguish TEDs and TSDs because the size of all observed TD-related hexagonal etch pits is quite close, which has a continuous distribution between 8.1 µm and 9.7 µm. Kallinger *et al.* reported that it is impossible to distinguish TD types by the size and shape of etch pits for highly doped n-type 4H-SiC substrates and epilayer, as the size distributions of TED and TSD related etch pits are overlapping.[21] In the epi-structure of the APD arrays fabricated in this work, the total thickness of the top p^+, p and i layers above the n^+ contact layer is only $\sim$1 µm. Then during the molten KOH etching process, the etch front would quickly reach the n^+ layer. This may explain why no apparent size difference of TED etch pits and TSD etch pits is observed. In addition, the reason why a very small number of BPD related etch pits are observed is that under current etch conditions, the etch front should lie in the upper region of the n^+ layer, while most BPDs have been converted into TDs during the initial 1–2 µm n^+ layer growth.

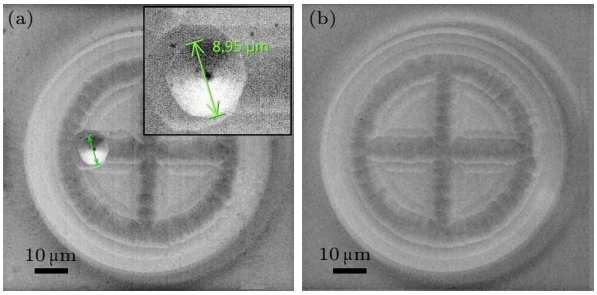

Fig. 4. Typical SEM images of a leaky APD (a) and a normal APD (b) after molten KOH etching. A TD-related hexagonal etch pit is observed on the leaky APD.

Figure 4 shows the typical SEM images of a leaky APD and a normal APD after molten KOH etching, respectively. An etch pit is observed within the mesa region of the leaky APD while no etch pit is found in the normal APD. Based on microscopic observation of 650 etched APD samples, it is found that all leaky APDs contain at least one TD, suggesting that TD is the main cause for the APD performance degradation. The enhanced leakage current near breakdown and higher DCR should be due to trap-assisted tunneling through TDs,[22–24] while distortion of electric field near TD regions could explain the slightly reduced breakdown voltage.[25] Meanwhile, as has been revealed in Fig. 2(a), TDs have nearly no impact on leakage current at low and medium reverse bias region, which agrees with past leakage current study of SiC p–n junction diodes.[26–28] This result suggests that fabrication of large area conventional SiC p–i–n photodiodes is feasible while the size of SiC APDs is seriously limited by dislocation density of SiC epi-structures. Interestingly, it is found that a very small fraction of normal devices could also contain a TD within their active region. That is, all leaky devices must contain at least one TD, while a TD within the active region does not necessarily lead to apparent APD degradation. Here long term reliability is not considered in performance evaluation. Based on the correlation study of up to 650 APD devices, as shown in Fig. 5, the relationship between TD and APD performance can be divided into three categories: normal APDs without TD (named as type A), leaky APDs with TD (named as type B) and "apparently normal" APDs with TD (named as type C). Their ratios are 89%, 9.5% and 1.5%, respectively. Through statistical analysis, at a confidence value of 95%, the confidence interval that a TD would induce apparent device degradation is [76.06%, 89.94%]. Thus, based on this study, one can claim with good confidence that even a single TD within the SiC APD active region would induce device performance degradation. Assuming that a leaky device or an "apparently normal" device has only one TD within the APD active region and the TD density of the SiC epi-layer is $2 \times 10^3\,\mathrm{cm}^{-2}$, a device yield of 87.5% could be produced if the APD diameter is 90 µm, which is consistent with the experimental yield of 89%.

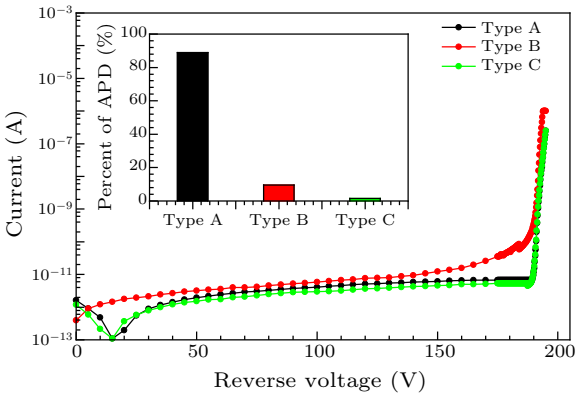

Fig. 5. Typical I–V curves of three types of SiC APDs. The inset shows the statistical ratios of the three types of APDs.

As for reason why a very small number of TDs seem to be not fatal to device performance, the underlying mechanism may be related to the detailed microstructure of these TDs. As has been mentioned, in this work it is impossible to definitely distinguish TSDs and TEDs only based on the size of etch pits. To judge whether or not these non-fatal TDs are really special, more advanced characterization techniques such as transmission electron microscopy or synchrotron x-

ray topography have to be applied. Moreover, Fujiwara *et al.* put forward the concept of nano-scale pits above TDs, and suggested that the main impact on dark current is the surface morphology of the nano-scale pits rather than the presence of TDs.[29–31] Even these special TDs have no impact on apparent device performance, they may cause reliability issues. Further investigations are under way and will be reported elsewhere.

In summary, 128-pixel 4H-SiC APD linear arrays have been fabricated to study the impact of TDs on electrical and single photon detection performance of SiC APDs. Based on a statistical study of 650 APD devices, a strong correlation is established to link the presence of a single dislocation and performance degradation of APD devices. Nowadays, state-of-the-art 4H-SiC substrates and epitaxy technologies could provide 4H-SiC epi-structures with TD density down to 1000–2000 cm^{-2}, which should be low enough for discrete small diameter APD devices. However, for large-pixel-number focal plane array development, current TD density level is still so high that high percentage of bad pixels would be unavoidable. Thus, for realizing high quality weak UV imaging based on SiC APD focal plane arrays, defect density within the SiC APD epi-structure has to be further considerably reduced.

References

[1] Razeghi M 2002 *Proc. IEEE* **90** 1006
[2] Kumamoto Y, Fujita K, Smith N I and Kawata S 2016 *Biomed. Opt. Express* **7** 158
[3] Chen H, Liu K, Hu L, Al-Ghamdi A A and Fang X 2015 *Mater. Today* **18** 493
[4] Wang Y, Qian Y and Kong X 2018 *IEEE Photon. J.* **10** 7000919
[5] Hadfield R H 2009 *Nat. Photon.* **3** 696
[6] Campbell J C 2016 *J. Lightwave Technol.* **34** 278
[7] Yi X, Xie S, Liang B, Lim L W, Cheong J S, Debnath M C, Huffaker D L, Tan C H and David J P R 2019 *Nat. Photon.* **13** 683
[8] Chunnilall C J, Degiovanni I P, Kueck S, Mueller I and Sinclair A G 2014 *Opt. Eng.* **53** 081910
[9] Powell A R and Rowland L B 2002 *Proc. IEEE* **90** 942
[10] Vert A, Soloviev S and Sandvik P 2009 *Phys. Status Solidi A* **206** 2468
[11] Rupp R, Treu M, Türkes P, Beermann H, Scherg T, Preis H and Cerva H 2005 *Mater. Sci. Forum* **483** 925
[12] Song H and Sudarshan T S 2013 *J. Cryst. Growth* **371** 94
[13] Stahlbush R E, Vanmil B L, Myers-Ward R L, Lew K K, Gaskill D K and Eddy Jr C R 2009 *Appl. Phys. Lett.* **94** 041916
[14] Chong E, Park B H, Cha H Y, Choi K and Lee D H 2018 *IEEE Photon. Technol. Lett.* **30** 899
[15] Morisette D T and Cooper Jr J A 2002 *Mater. Sci. Forum* **389** 1133
[16] Berechman R A, Skowronski M and Zhang Q 2009 *J. Appl. Phys.* **105** 074513
[17] Zhou D, Liu F, Lu H, Chen D Z, Ren F, Zhang R and Zheng Y 2014 *IEEE Photon. Technol. Lett.* **26** 1136
[18] Su L, Cai X, Lu H, Zhou D, Xu W, Chen D, Ren F, Zhang R, Zheng Y and Li G 2019 *IEEE Photon. Technol. Lett.* **31** 447
[19] Fujibayashi H, Ito M, Ito H, Kamata I, Naito M, Hara K, Yamauchi S, Suzuki K, Yajima M, Mitani S, Suzuki K, Aoki H, Nishikawa K, Kozawa T and Tsuchida H 2014 *Appl. Phys. Express* **7** 15502
[20] Song H, Deng J, Dai Q, Shi Z and Yu L 2016 *IEEE Trans. Electron Devices* **63** 4845
[21] Kallinger B, Polster S, Berwian P, Friedrich J, Müller G, Danilewsky A N, Wehrhahn A and Weber A D 2011 *J. Cryst. Growth* **314** 21
[22] Yang S, Zhou D, Cai X, Xu W, Lu H, Chen D, Ren F, Zhang R, Zheng Y and Wang R 2017 *IEEE Trans. Electron Devices* **64** 4532
[23] Vilà A, Trenado J, Arbat A, Comerma A, Gascon D, Garrido L and Dieguez A 2011 *Sens. Actuators A* **172** 181
[24] Bai X, Guo X, Mcintosh D C, Liu H and Campbell J C 2007 *IEEE J. Quantum Electron.* **43** 1159
[25] Chynoweth A G and Pearson G L 1958 *J. Appl. Phys.* **29** 1103
[26] Zhao F, Islam M M, Daas B K and Sudarshan T S 2010 *Mater. Lett.* **64** 281
[27] Berechman R A, Skowronski M, Soloviev S and Sandvik P 2010 *J. Appl. Phys.* **107** 114504
[28] Neudeck P G, Huang W and Dudley M 1998 *Solid-State Electron.* **42** 2157
[29] Katsuno T, Watanabe Y, Fujiwara H, Konishi M, Naruoka H, Morimoto J, Morino T and Endo T 2011 *Appl. Phys. Lett.* **98** 222111
[30] Fujiwara H, Naruoka H, Konishi M, Hamada K, Katsuno T, Ishikawa T, Watanabe Y and Endo T 2012 *Appl. Phys. Lett.* **100** 242102
[31] Fujiwara H, Naruoka H, Konishi M, Hamada K, Katsuno T, Ishikawa T, Watanabe Y and Endo T 2012 *Appl. Phys. Lett.* **101** 042104